Atmospheric soluble dust records from a Tibetan ice core: Possible climate proxies and teleconnection with the Pacific Decadal Oscillation

B. Grigholm,[1] P. A. Mayewski,[1] S. Kang,[2,3] Y. Zhang,[2] S. Kaspari,[1,4] S. B. Sneed,[1] and Q. Zhang[2]

[1] In autumn 2005, a joint expedition between the University of Maine and the Institute of Tibetan Plateau Research recovered three ice cores from Guoqu Glacier (33°34′37.8″N, 91°10′35.3″E, 5720 m above sea level) on the northern side of Mt. Geladaindong, central Tibetan Plateau. Isotopes ($\delta^{18}O$), major soluble ions (Na^+, K^+, Mg^{2+}, Ca^{2+}, Cl^-, NO_3^-, SO_4^{2-}), and radionuclide (β-activity) measurements from one of the cores revealed a 70-year record (1935–2005). Statistical analysis of major ion time series suggests that atmospheric soluble dust species dominate the chemical signature and that background dust levels conceal marine ion species deposition. The soluble dust time series have interspecies relations and common structure (empirical orthogonal function (EOF) 1), suggesting a similar soluble dust source or transport route. Annual and seasonal correlations between the EOF 1 time series and National Centers for Environmental Prediction/National Center for Atmospheric Research reanalysis climate variables (1948–2004) suggest that the Mt. Geladaindong ice core record provides a proxy for local and regional surface pressure. An approximately threefold decrease of soluble dust concentrations in the middle to late 1970s, accompanied by regional increases in pressure and temperature and decreases in wind velocity, coincides with the major 1976–1977 shift of the Pacific Decadal Oscillation (PDO) from a negative to a positive state. This is the first ice core evidence of a potential teleconnection between central Asian atmospheric soluble dust loading and the PDO. Analysis of temporally longer ice cores from Mt. Geladaindong may enhance understanding of the relationship between the PDO and central Asian atmospheric circulation and subsequent atmospheric soluble dust loading.

1. Introduction

[2] Atmospheric dust aerosols play a significant role in the global climate system influencing the Earth's radiative budget and albedo by scattering and absorbing incoming shortwave (solar) radiation [*Claquin et al.*, 1999; *Tegen et al.*, 1996] and acting as cloud condensation nuclei [*Pruppacher and Klett*, 1978]. Atmospheric dust particles are also influential in atmospheric chemical reactions, as a source of nutrients for biological systems [*Li-Jones and Prospero*, 1998; *Zhang and Carmichael*, 1999], and can have serious impacts on human health, agriculture, and economics. Therefore, the reconstruction of past atmospheric dust concentrations is important in understanding variations in climate and environmental conditions. Ice core records provide the most direct and detailed way to investigate preinstrumental temporal variations of atmospheric dust and extrapolate paleoclimatic and paleoatmospheric conditions. Central Asia, one of the Northern Hemisphere's major dust source regions, is a prime location for the retrieval of ice cores because it contains several of the Earth's highest mountain ranges (e.g., Himalayas, Pamirs, Hindu Kush, Tien Shan, Altai) and, the Tibetan Plateau (TP), which spans ~2.5 million km^2 at an average elevation of ~4000 m. It is at these elevations that middle- to low-latitude ice core environmental records are best preserved. Since the early 1980s ice core research has been conducted in carefully selected high-altitude sites [*Aizen et al.*, 1996, 2004; *Kang et al.*, 2001, 2002a, 2002b; *Kreutz et al.*, 2001; *Kreutz and Sholkovitz*, 2000; *Lyons and Mayewski*, 1983; *Mayewski et al.*, 1983, 1984; *Qin et al.*, 2000, 2002; *Thompson et al.*, 1989, 1993, 1995, 1997, 2000; *Wake et al.*, 1990, 1993, 1994] providing high-resolution paleoclimate

---

[1]Climate Change Institute, Department of Earth Sciences, University of Maine, Orono, Maine, USA.
[2]Institute of Tibetan Plateau Research, Chinese Academy of Sciences, Beijing, China.
[3]Also at State Key Laboratory of Cryospheric Science, Chinese Academy of Sciences, Lanzhou, China.
[4]Also at Department of Geological Sciences, Central Washington University, Ellensburg, Washington, USA.
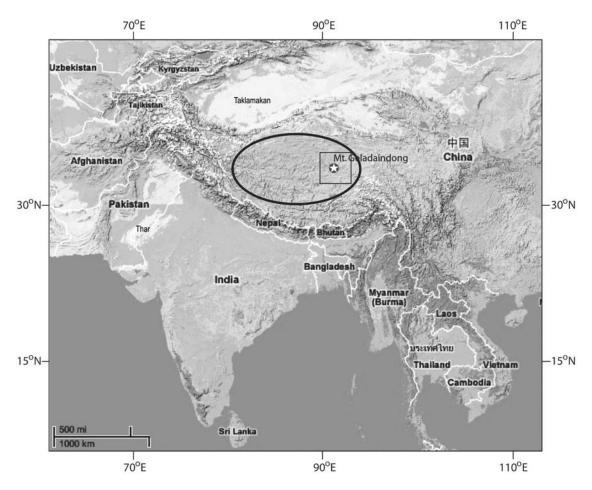
Figure 1. Location map of study area. Star represents drill site. Square represents National Centers for Environmental Prediction (NCEP)/National Center for Atmospheric Research (NCAR) reanalysis grid. Area within black oval approximately represents areas covered by calcisols, solonchaks, and leptosols [*Institute of Soil Science of Academia Sinica*, 1985]. Examples of distal dust source regions include Taklamakan and Thar deserts (Google Maps image).

records that have greatly added to the understanding of the Asian climate during the late Holocene.

[3] Here we present a 70-year atmospheric soluble dust deposition record (1935–2004) developed from a Mt. Geladaindong ice core located in the Tanggula Mountains on the TP (Figure 1) and investigate the spatial and temporal relationships between ice core chemistry and related climate parameters (pressure, wind velocity, precipitation, and temperature) that impact atmospheric soluble dust concentrations on local and regional scales. We also investigate the potential of the Mt. Geladaindong ice core chemistry to serve as a climate proxy for preinstrumental periods and explore a potential teleconnection between TP atmospheric soluble dust concentrations and the Pacific Decadal Oscillation (PDO).

2. Study Region

[4] The modern TP climate is strongly influenced by polar air masses from the Arctic, continental air masses from central Asia, and equatorial-maritime air masses from the Indian and Pacific Oceans [*Bryson*, 1986]. Its massive size splits the upper-level westerlies and effects surface and upper-level pressure distributions. Northern regions of

the TP are dominated by the interaction of Siberian anticyclones and westerly cyclones [*Aizen et al.*, 1996], while southern regions are dominated by westerly cyclones and the Asian monsoon. Seasonal heating and cooling over northern Asia creates large pressure differences between the Asian continent and the Indian Ocean and generates conditions that form the South Asian Monsoon (or the Indian Monsoon), the largest seasonal reversal of wind patterns and precipitation regimes on Earth. The Tanggula Mountains, central TP, are thought to mark the northern extent of the Indian Monsoon, while regions further north receive moisture provided by continental water recycling [*Tian et al.*, 2001].

[5] Transitions in atmospheric circulation over the TP occur in the spring and in the autumn. During the autumn the westerly wind velocity over the plateau intensifies reaching a maximum in winter. Coupling between upper level wind patterns and surface winds during surges of cold continental air masses and the polar jet stream are thought to generate cyclones responsible for dust storms. During the spring the westerlies begin to migrate to the north and wind velocities decrease reaching minimum values during the summer.

Table 1. Statistical Summary of Mt. Geladaindong Major Soluble Ions, Procedural Blanks, and Procedural and Instrument Detection Limits[a]

Ion	Mean	Median	SD	Min.	Max.	%TC[b]	CMDS Blank[c]	CMDS DL (3σ)	IDL
Na^+	286.0	132.1	494.8	<IDL	4846	11.7	<IDL	<IDL	0.62
K^+	28.3	16.4	38.6	<IDL	337	1.5	<IDL	<IDL	0.64
Mg^{2+}	87.0	52.0	114.8	<IDL	976	4.6	8.6	1.5	0.12
Ca^{2+}	928.4	489.6	1501.6	<IDL	16698	43.4	50.7	52.2	0.24
Cl^-	336.0	175.2	531.8	<IDL	4727	15.5	7.6	3.3	0.52
NO_3^-	183.5	107.5	252.9	<IDL	2154	9.5	<IDL	<IDL	0.48
SO_4^{2-}	379.4	156.4	788.5	<IDL	15368	13.5	<IDL	<IDL	2.32

[a]Values are in micrograms per liter. Abbreviations are as follows: CMDS, continuous melter with discrete sampling; DL, detection limit; IDL, instrument detection limit.
[b]Percentage of total ion concentration of mean Mt. Geladaindong sample.
[c]Mean value.

[6] The major central Asian dust sources are located in the deserts of northern and northwestern China and contribute ~100–800 Tg dust yr^{-1} [*Laurent et al.*, 2006; *Zhang et al.*, 1997]. Springtime cyclonic activity and winter temperatures in these regions result in peaks in dust activity between mid-February and late May, with a strong maximum in late April to early May [*Merrill et al.*, 1989; *Qian et al.*, 2002]. On the TP, a dust source upwind of the Chinese Loess Plateau, atmospheric dust is generated from local soils on the plateau, while other materials are transported into the region from long-distance sources. Dust from the TP is suggested to be composed of ~70% local and 25% distant material [*Zhang et al.*, 1996]. Abundant local soils include calcisols, solonchaks, and leptosols [*Institute of Soil Science of Academia Sinica*, 1985]. Other areas with entrainable materials include dried lake sediments, which are scattered across the TP [*Li et al.*, 2007]. These potential dust sources are located all around Mt. Geladaindong, however, considering westerly circulation most dust aerosols are probably originating to the west of Mt. Geladaindong. Comparison between back trajectory models (HY-SPLIT 4) and microparticle concentrations and fluxes from several Mt Geladaindong snow pits suggest that dust aerosols are mainly coming from northwestern areas of the TP [*Zhang et al.*, 2008]. Distal dust sources may derive from the arid regions in northern China (e.g., Taklmakan desert) or other deserts in northern India, Pakistan, or central Asia [*Zhang et al.*, 2001; *Liu et al.*, 2008]. Weather station records on the TP show that dust activity occurs primarily between November and May [*Han et al.*, 2004]. The amount that TP dust sources contribute to long-distance atmospheric dust transport is still unknown. Research suggests that the atmospheric loading of Asian dust originating from the deserts of north and northwestern China dominate long-distance transport when compared to dust input from the TP [*Zhang et al.*, 2001]. However, recent study suggests that due to the high elevation of the TP, entrainment of dust may regularly reach upper tropospheric transport pathways and therefore contribute more to long-distance Asian dust transport than previously thought [*Fang et al.*, 2004].

3. Methodology
3.1. Retrieval and Analysis of the Mt. Geladaindong Ice Core
[7] During October and November 2005, an ice core drilling expedition was conducted on the Guoqu Glacier located on the northern slope of Mt. Geladaindong (33.58°N, 91.17°E, 5720 m above sea level) in the Tanggula Mountains located in the center of the TP (Figure 1). Three ice cores were recovered (74 m, 147 m, and 22 m) from the flat firn basin in the accumulation zone of Guoqu Glacier using the Cold and Arid Regions Environmental and Engineering Research Institute (CAREERI) electromechanical drill. The ice cores were transported frozen to the State Key Laboratory of Cryospheric Science in Lanzhou, China. This study focuses on the 74 m core.

[8] Preparations for sampling the core involved cutting the ice core sections longitudinally into quarters and scraping all ice surfaces with stainless steel scalpels precleaned with deionized (DI) water (>18.2 MΩ). The ice core was melted at the State Key Laboratory of Cryospheric Science in Lanzhou, China using a continuous melter with discrete sampling (CMDS) system with a nickel 270 (>99.99% Ni) melt head [*Osterberg et al.*, 2006]. Continuous melter blanks and detection limits (3σ) were calculated from DI water blanks passed through the entire CMDS system throughout the melting campaign (Table 1). Na^+, K^+, NO_3^-, and SO_4^{2-} had CMDS detection limits below the instrumental detection limits of the ion chromatograph. Detection limits of Cl^-, Mg^{2+}, and Ca^{2+} were approximately 1%, 2% and 6% of mean concentration values, respectively. Sample resolution was 3–5 cm yielding 23 samples yr^{-1} on average. A total of 1621 coregistered samples were collected into high-density polyethylene (HDPE) vials and precleaned (with DI water) polypropylene (PP) vials for analysis of stable isotope ratios ($\delta^{18}O$) and soluble ion concentrations (Na^+, K^+, Ca^{2+}, Mg^{2+}, Cl^-, NO_3^-, SO_4^{2-}). Samples were analyzed at the University of Maine for major soluble ion concentration using Dionex DX-500 ion chromatographs. $\delta^{18}O$ was analyzed via a MAT-253 at the Institute of Tibetan Plateau Research, Chinese Academy of Science. The β-activity was analyzed at ~1 m resolution (~1 sample yr^{-1}) at the Maine State Lab in Augusta.

3.2. Dating the Ice Core
[9] The Mt. Geladaindong depth-age scale is presented in Figure 2a. Annual dating was calibrated using the 1963 nuclear test horizon (marked as a β-activity peak) as an absolute age marker complemented by a multiparameter annual layer-counting methodology using subannually resolved stable isotopes and major soluble ions. The maximum β-activity peak was selected as 1963 to reflect the maximum fallout of nuclear weapons testing [*Anspaugh et al.*, 2000]. The mean annual accumulation rate (0.53 m water
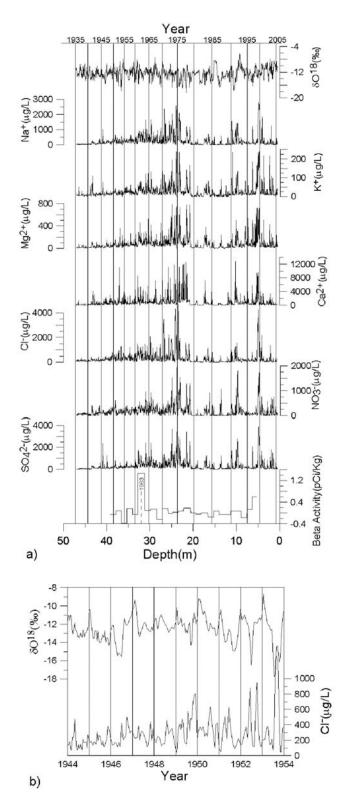
Figure 2. (a) Mt. Geladaindong ice core depth−age scale. (b) Annual layer dating based on seasonality of summer monsoon $\delta^{18}O$ depleted precipitation and late autumn−spring seasonality of major soluble ion dust species (Cl^-).

equivalent (weq.)) at the Mt. Geladaindong site allows for the preservation of distinct seasonal cycles in chemical species. On the basis of the results of onsite snow pit studies individual years were selected by identifying the

seasonality of $\delta^{18}O$ depleted summer monsoon precipitation and late autumn-spring peaks in major ion dust species (Na^+, K^+, Ca^{2+}, Mg^{2+}, Cl^-, NO_3^-, and SO_4^{2-}) [Kang et al., 2007] (Figure 2b). It is important to note that not all of the major ions in the snow pits showed the same patterns as might be expected if the record had been postdepositionally altered. Ca^{2+}, for example, in the snow pits and the ice core show independent as well as shared peaks with Na^+, K^+, Mg^{2+}, Cl^-, and SO_4^{2-} during autumn-spring. The variation in chemistry concentration peaks may suggest the influence of different dust source regions at different times of the year. In addition, snow pit studies showed that the common seasonality of major soluble ions was supported by very similar trends in microparticles (concentration and flux) [Zhang et al., 2008]. Dating of the entire core was not possible due to a sudden loss in overall ion concentrations and variability at ∼50 m. The loss of an ion signal suggests the past presence of meltwater, which was discovered during drilling at 74 m. The 147 m ice core encountered no water and preliminary major ion analysis revealed no loss of ion variability throughout the core. Upper sections of both ice cores share major soluble ion trends and variability. This study is focused on the major ion time series (1935−2004) from the top 47 m of the ice core.

4. Results and Discussion

4.1. Major Soluble Ion Time Series

[10] Major soluble ion concentration records are shown in Figure 2a. Each record consists of 1635 samples, averaging 23 samples yr^{-1}. A statistical summary of the major ions is provided in Table 1; presenting mean, median, standard deviation (SD), minimum, and maximum concentration values. Major soluble ion annual median concentrations (conc.) and annual median fluxes (flux) were calculated to determine any accumulation biases. Time series of major soluble ion$_{conc.}$ and major soluble ion$_{flux}$ displayed overall very similar trends, although some differences are apparent (Figure 3). Because exact dust input timing is unknown (e.g., dry versus wet deposition) one (concentration or flux) time series cannot more accurately be selected, therefore, both annual median concentration and flux of major soluble ion series are investigated. Individual sample data, annual median concentration and annual median flux correlations indicate strong positive relationships among major ions suggesting that major ions may originate from a common dust source or share common atmospheric transport pathways (Table 2). Additional, separate Empirical Orthogonal Function (EOF) analysis was conducted on major soluble ion $_{conc.}$ and major soluble ion $_{flux}$ data to characterize covariability of the time series and investigate potential annual interspecies associations (e.g., transport pathways and provenance; Table 3). EOF analysis also produced new time series that represent the covariability of different variables. Hereon the *conc.* and *flux* subscript refers in singular reference to two separate time series (e.g., EOF 1 $_{conc. and flux}$). EOF 1 $_{conc. and flux}$ accounted for ∼84– 86% of the total variance in the major ion series. The strong relationship among the major ion species suggests that most of the major ions have a common source or similar atmospheric transport pathways. Crustal aerosols represent the dominant component of the TP atmosphere
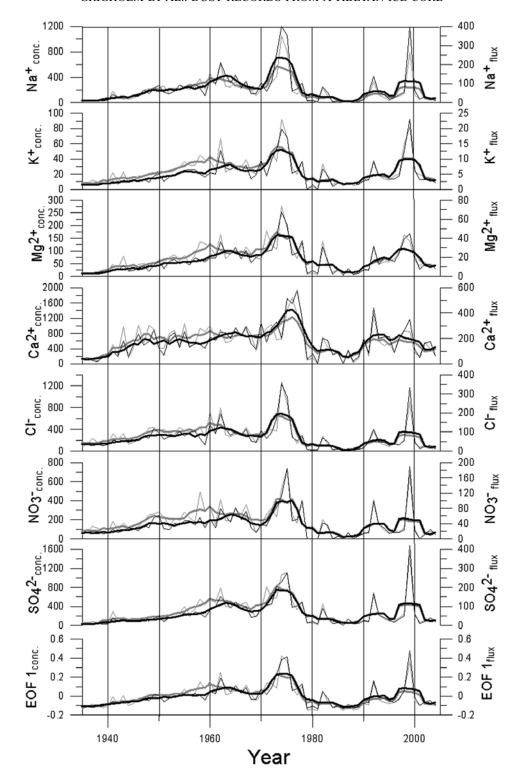
Figure 3. Mt. Geladaindong major soluble ion time series$_{\text{conc. and flux}}$: annual concentration (μg/L; thin line) and annual flux (mg m^{-2} yr^{-1}; shaded line). Bold lines represent 5-year running means.

[*Cong et al.*, 2007; *Li et al.*, 2007; *Zhang et al.*, 2001]. Therefore, EOF 1 most likely represents a soluble dust source from the arid to semiarid regions on the TP. Potential sources of soluble Na$^+$, Cl$^-$, K$^+$, Ca^{2+}, Mg^{2+}, and SO$_4^{2-}$ are evaporite rock minerals (e.g., calcite, dolomite, gypsum, anhydrite, halite, and potassium/magnesium salts) from soils (e.g., calcisols, solonchaks, and leptosols), sedimentary rocks

(e.g., limestone and dolomite), and/or dried lake sediments that are common in the Mt. Geladaindong region [*Institute of Soil Science of Academia Sinica*, 1985; *Li et al.*, 2007, 2008; *Liu et al.*, 2008]. EOF 2 $_{\text{conc. and flux}}$ represents ~8% of the total variance in major ion series and is dominated by Ca^{2+} $_{\text{conc. and flux}}$ (~44–47%). The difference in the Ca$^{2+}_{\text{conc. and flux}}$ time series relative to the other

Table 2. Correlation Coefficients Between Major Ions in Mt. Geladaindong Core[a]

	Na^+	K^+	Mg^{2+}	Ca^{2+}	Cl^-	NO_3^-	SO_4^{2-}
Na^+	–	0.86 (0.91, 0.94)	0.66 (0.88, 0.87)	0.46 (0.71, 0.58)	0.93 (0.96, 0.97)	0.78 (0.89, 0.92)	0.83 (0.96, 0.94)
K^+		–	0.83 (0.91, 0.92)	0.52 (0.71, 0.65)	0.81 (0.87, 0.91)	0.75 (0.81, 0.88)	0.80 (0.92, 0.93)
Mg^{2+}			–	0.65 (0.81, 0.71)	0.60 (0.85, 0.82)	0.70 (0.88, 0.81)	0.67 (0.90, 0.85)
Ca^{2+}				–	0.44 (0.66, 0.54)	0.40 (0.79, 0.70)	0.40 (0.76, 0.67)
Cl^-					–	0.71 (0.88, 0.89)	0.78 (0.90, 0.89)
NO_3^-						–	0.76 (0.87, 0.93)
SO_4^{2-}							–

[a]Correlation coefficients are of individual sample data, and parentheses indicate annual median concentrations and annual median flux. All coefficient values have $p > 0.001$.

major ion time series suggests that there may be a secondary dust source dominated by Ca^{2+} that has varied annually from the EOF $1_{conc.\ and\ flux}$ dust source. This source may possibly be a calcite source as no other ions load on EOF $2_{conc.\ and\ flux}$. Although marine air masses do penetrate the Geladaindong region during the summer monsoon season, the lack of an EOF directly representing sea salt ions suggests that the ion input of marine air masses is concealed by abundant crustal inputs (e.g., soluble dust). Any anthropogenic ion inputs, (e.g., HCl [*Shrestha et al.*, 2002]), are also assumed to be concealed by crustal inputs.

[11] To emphasize long-term atmospheric major soluble ion $_{conc.\ and\ flux}$ trends, 5-year running means were calculated (Figure 3). Between 1935 and the early 1970s all ions display a gradual rise with slight undulations in concentrations followed by a sharp rise in the mid 1970s. An abrupt drop in concentrations and a low-dust period during the 1980s follows this concentration/flux peak. Comparison between 10-year periods before and after the mid-1970s peak in dust concentrations indicate an approximately two- to threefold decrease in concentration/flux in all major ions. During the 1990s concentration/flux levels increased with a major peak in 1999, followed by lower levels to the present. Ca^{2+} $_{conc.\ and\ flux}$ generally has the same trend as the other ions, however, its mid-1970s peak and subsequent drop in concentrations occurs 2 years later. Another prominent feature in the Ca^{2+} $_{conc.\ and\ flux}$ not seen in the other ion records is the sharp increase during the early 1990s. These differences in the Ca^{2+} concentration time series, as suggested by EOF analysis, support the presence of an additional Ca^{2+} source and/or transport route.

4.2. EOF $1_{conc.\ and\ flux}$ and National Centers for Environmental Prediction/National Center for Atmospheric Research Reanalysis Climate Parameters

[12] EOF $1_{conc.}$ and EOF 1_{flux} were selected for comparison with NCEP/NCAR reanalysis climate parameters because they represent ~84–86% of the variance in the major ion series$_{conc.\ and\ flux}$ and most likely originate from similar sources and/or transport pathways. A NCEP/NCAR reanalysis $2.5° \times 2.5°$ grid (Figure 1) overlapping the Mt. Geladaindong site provides data time series (1948–2004) for surface temperature, pressure, scalar wind velocity (SWV), and precipitation [*Kalnay et al.*, 1996]. Comparisons between atmospheric aerosols and climate parameters can help determine potential proxies and relationships that can be used to reconstruct climate in the preinstrumental era. It is important to note, that the coarse resolution of NCEP/NCAR reanalysis cannot resolve all of the complex

topography that may influence small-scale climate on the TP. However, *Xie et al.* [2007] investigated the reliability of NCEP/NCAR reanalysis in the Himalayan/Tibetan Plateau region and found that much of the synoptic-scale climate variability was captured.

[13] Variations in annual averages and 5-year running means for surface-level climate variables (precipitation, temperature, SWV, and pressure) from 1948 to 2004 in the Mt. Geladaindong region, along with EOF $1_{conc.\ and\ flux}$ (annual median and 5-year running mean) from 1935 to 2004, are displayed in Figure 4. Surface SWV is calculated from the NCEP/NCAR reanalysis parameters surface zonal wind velocity (u) and surface meridional wind velocity (v) [*Jacobson*, 2005].

[14] Corresponding abrupt shifts in the mid-1970s are prominent between EOF $1_{(conc.\ and\ flux)}$, pressure, and SWV. Trends in pressure, a potential indicator of cyclonic storm activity, show a general negative relationship with EOF $1_{(conc.\ and\ flux)}$ both before and after the mid-1970s shift. The pre-mid-1970s lower-pressure period corresponds to higher values (i.e., higher soluble dust concentration/flux) of EOF $1_{(conc.\ and\ flux)}$, while the post-mid-1970s higher-pressure period corresponds to lower values (i.e., lower soluble dust concentration/flux) of EOF $1_{(conc.\ and\ flux)}$. The relationship is negative, indicating that during years of lower-pressure EOF $1_{(conc.\ and\ flux)}$ values are higher, most likely a result of more intense cyclonic storm activity as demonstrated by other ice core – climate calibrations in the Arctic, Antarctic, and subpolar regions [e.g., *Mayewski et al.*, 2004; *Kang et al.*, 2002a; *Kaspari et al.*, 2007]. Decreases in pressure for cyclonic features result in intensification of wind velocities and increased incorporation of chemistry over the land and sea. The assumption that pressure may indicate cyclonic storm activity is additionally supported by *Qian et al.* [2002] who reported a rapid decrease in cyclonic activity between 1976 and the late

Table 3. Empirical Orthogonal Function Analysis of Major Soluble Ions$_{conc.\ and\ flux}$[a]

	EOF 1		EOF 2	
	Concentration	Flux	Concentration	Flux
Na^+	93.82	91.61	−4.41	−6.02
K^+	93.40	92.07	−0.66	−0.23
Mg^{2+}	85.72	84.18	0.75	0.53
Ca^{2+}	54.23	51.81	44.47	46.56
Cl^-	88.66	86.48	−6.04	−5.02
NO_3^-	90.34	88.84	0.00	0.02
SO_4^{2-}	93.02	90.42	−0.29	−0.25
Total	85.60	83.63	8.09	8.44

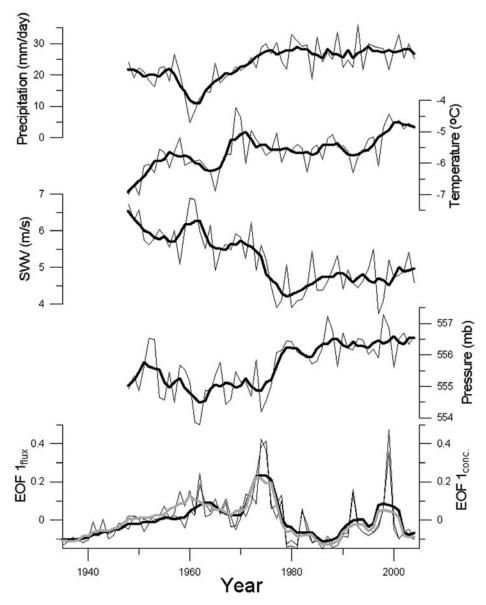[a]EOF, empirical orthogonal function.

Figure 4. NCEP/NCAR reanalysis annual average surface climate parameters (precipitation, temperature, scalar wind velocity, pressure) and empirical orthogonal function (EOF) $1_{conc. \text{ and flux}}$. versus time. Five-year running mean (bold lines) and 1-year mean (thin lines).

1990s in northern China coinciding with the abrupt rise and relatively higher values of pressure in the Mt. Geladaindong region. SWV trends display a consistent association with pressure/storm strength showing a positive relationship with EOF $1_{(conc. \text{ and flux})}$ suggesting that greater wind velocity results in more aerosols entrained into the atmosphere. Temperature and precipitation display shifts in trends prior to the mid-1970s EOF $1_{(conc. \text{ and flux})}$ shift. Fluctuations in temperature and precipitation will have impacts on land surface properties that affect the potential of dust entrainment in the atmosphere (i.e., soil moisture).

[15] EOF analysis and linear correlations were used to quantify potential annual relationships between EOF $1_{(conc. \text{ and flux})}$ with climate variables (Table 4). EOF $1_{(conc. \text{ and flux})}$ were compared to annual averages (January–December) and to the annual averages of the months of primary dust storm activity (November–May), hereon referred to as dust

months (DM). The DM were selected based on multiple weather station monthly dust storm records in the Mt. Geladaindong region [*Han et al.*, 2004]. Annual averages of climate variables were also examined because although dust activity is reduced during the incursion of the summer monsoon season, major dust events can still occur [*Huang et al.*, 2007].

[16] EOF analysis was conducted on two series at a time (e.g., EOF $1_{conc.}$ and pressure). The first component (EOF 1) expresses the dominant similarity (positive correlation) or dissimilarity (negative correlation) between the two series and estimates the common association between the series. For pressure (DM and annual) EOF analysis reveals that 64% and 67% of the variance in the EOF $1_{conc.}$ and pressure series is represented by the first EOF (negative correlation), respectively. The EOF 1_{flux} and pressure (DM and annual) series analysis reported 69% and 74% of the variance

Table 4. EOF Analysis and Linear Correlation of EOF $1_{conc. \text{ and flux}}$[a]

Series	Concentration			Flux		
	EOF 1 (%)	r	p value	EOF 1 (%)	r	p value
Annual pressure	67.34	−0.35	<.01	74.52	−0.49	0.0001
DM pressure	64.71	−0.29	<.03	69.47	−0.39	<0.003
Annual SWV	56.80	0.14		64.83	0.30	<.03
DM SWV	54.55	0.09		61.24	0.22	
Annual precipitation	56.92	−0.14		63.79	−0.28	<.04
DM precipitation	50.09	0.00		53.41	−0.07	
Annual temperature	50.05	0.00		55.74	−0.11	
DM temperature	50.09	−0.02		57.73	−0.13	
PDO index	70.88	−0.42	<.001	72.86	−0.46	<.0001

[a]Abbreviations are as follows: DM, dust month; EOF, empirical orthogonal function; PDO, Pacific Decadal Oscillation; SWV, scalar wind velocity. P values > 0.05 are not given.

(negative correlation), respectively. On the basis of the probability of red noise series (Monte Carlo estimation), *Meeker and Mayewski* [2002] reported that shared variance values exceeding 64% is equivalent to p < 0.01. The correspondence between annual pressure and the potential glaciochemical proxy (EOF $1_{conc. \text{ and flux}}$) is shown in Figure 5 (the first common component is shown as dashed gray line). Linear correlations also reported significant values for pressure (all reported p values are two tail). Pressure exhibited the strongest linear correlations with EOF 1_{flux} (annual: $r = -0.49$, $p = 0.0001$, $n = 57$; DM: $r = -0.39$, $p < 0.003$, $n = 57$) and slightly weaker correlations with EOF $1_{conc.}$ (annual: $r = -0.35$, $p < 0.01$, $n =$

57; DM: $r = -0.36$, $p < 0.03$, $n = 57$). Spatial correlation of EOF $1_{flux \text{ and conc.}}$ with annual pressure is presented in Figure 6 demonstrating that EOF 1/pressure relationship is reflected throughout the TP. EOF analysis of EOF $1_{flux \text{ and conc.}}$ and the SWV time series show overall weaker correlations than pressure. EOF 1_{flux} and SWV share 61% (DM) and 65% (annual) of their variance (positive correlation), while EOF $1_{conc.}$ displayed 55% (DM) and 56% (annual) of their variance. Only EOF 1_{flux} reported significant values for SWV; EOF 1_{flux} (annual: $r = 0.3$, $p < 0.03$, $n = 57$). EOF analysis and linear correlation for precipitation report only significant values for EOF 1_{flux} and annual precipitation ($r =$

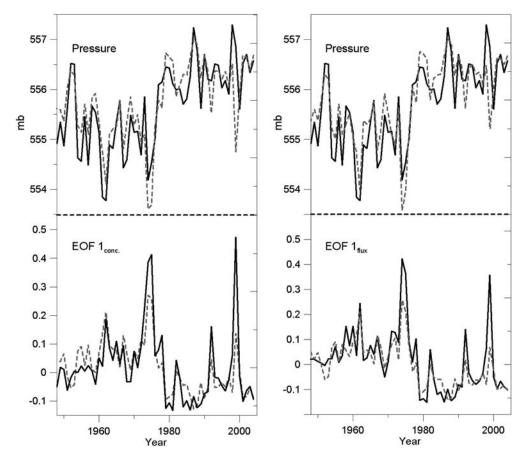**Figure 5.** Plots of annual pressure and EOF $1_{conc. \text{ and flux}}$ (solid line) and their common EOF 1 (dashed shaded line). For negative correlations (e.g., EOF $1_{conc.}$ and EOF 1_{flux}), the EOF is oriented inversely.
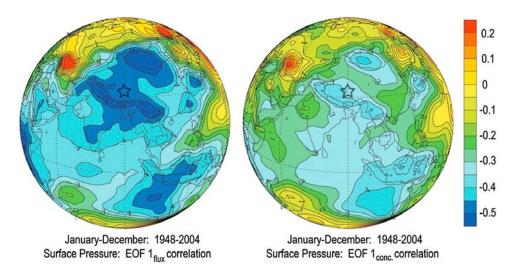
January–December: 1948-2004
Surface Pressure: EOF 1flux correlation

January–December: 1948-2004
Surface Pressure: EOF 1conc. correlation

Figure 6. NCEP/NCAR reanalysis spatial correlation with EOF $1_{conc.and\ flux}$ and January–December 1948–2004 surface pressure ($r = -0.34$, $p < 0.01$, $n = 57$). Stars represent the Mt. Geladaindong site.

0.28, $p < 0.04$, $n = 57$). No significant relationships were reported for temperature.

[17] The relationships reflected by EOF analysis and linear correlations suggest that pressure can best explain the annual variations in EOF $1_{conc.\ and\ flux}$. Pressure variations are indicative of atmospheric circulation and can provide natural aerosol (e.g., soluble dust) transport mechanisms to Mt. Geladaindong. As previously mentioned negative correlation between EOF 1 and pressure may reflect cyclonic storm activity. Lower-pressure years may suggest more intense or frequent cyclonic storm activity resulting in greater dust entrainment that subsequently leads to higher concentrations of major soluble ions. Higher-pressure years probably corresponding to weaker or less frequent cyclonic storm activity entrain less dust into the atmosphere and lead to lower concentrations of major soluble ions. Pressure shows significant correlation values for both EOF $1_{conc.}$ and EOF 1_{flux}. The stronger overall pressure correlations with EOF 1_{flux} could possibly suggest that flux values better reflect deposition conditions on the glacier. However, it is not clear which record actually is a better representation based on the uncertainties of the timing of dry and wet deposition. The overall stronger correlation values displayed by annual correlations relative to DM correlations may reflect the significant influence of cyclonic activity during the so-called non-DM (June–October) when atmospheric aerosols are at baseline concentrations.

[18] Although, SWV appears to show a multiyear positive relationship with EOF $1_{conc.\ and\ flux}$ (e.g., pre and post mid-1970s shift) annual correlations are not as robust as pressure, displaying only one significant positive relationship (annual EOF 1_{flux}). SWV is associated with cyclonic intensity, however, annual or monthly averages of wind strength may not necessarily reflect cyclonic activity thereby explaining overall weaker correlations. Precipitation correlations only yield significant values for annual EOF 1_{flux}, which could possibly reflect summer monsoon input (as DM report no significant correlations). The negative relationship between precipitation and EOF 1_{flux} may suggest that increased precipitation reduced summer atmospheric aerosols via scavenging and/or enhanced soil moisture that

limited entrainment areas over the summer or subsequent year.

[19] In addition to primary climate variables (i.e., pressure, SWV, temperature, and precipitation), atmospheric dust concentrations depend on the amount of available entrainable sediments. Therefore, the assessment of possible future atmospheric dust scenarios must consider land cover variations such as desertification, which can alter land surfaces to become more susceptible to dust entrainment. The TP is one of the most sensitive regions to global temperature change exceeding increase rates for the northern hemispheric and same latitude zones [*Liu and Chen*, 2000]. Recent warming has resulted in permafrost degradation throughout the TP and it is believed the loss of permafrost will lead to desertification [*Wang et al.*, 2000b]. In addition to climate variations, inappropriate land management practices on the TP have led to an alarming rate of land degradation and desertification [*Gong et al.*, 2004; *Wang et al.*, 2000a; *Zeng et al.*, 2003]. On the TP, over 62% of land is used for agriculture with 80% being used for livestock grazing and 19% for forestry [*Wu and Yang*, 2000]. Previous studies have shown that desert areas in China have increased by ~2% to ~7% since the 1950s [*Zhong*, 1999; *Zhu and Zhu*, 1999] and suggest that these new "desertified" areas would produce 10–40% more dust storms under the meteorological conditions of the 1950s. If the trend of land degradation and desertification continues on the TP, a present return to the pre-mid-1970s atmospheric conditions would most likely lead to higher atmospheric dust concentrations.

4.3. Potential Teleconnection to the Pacific Decadal Oscillation

[20] The Pacific Decadal Oscillation (PDO) is a long-lived (El Niño–like) interdecadal climate pattern that exists over the northern Pacific Ocean. It involves the location and intensity of large pools of warm and/or cold sea surface temperature anomalies in the central and eastern areas of the northern Pacific and has a periodicity of ~20–30 years. PDO reconstructions have been developed from tree ring records in western North America [*Biondi et al.*, 2001; *Cook*, 2002; *D'Arrigo et al.*, 2001; *Gedalof and Smith*,
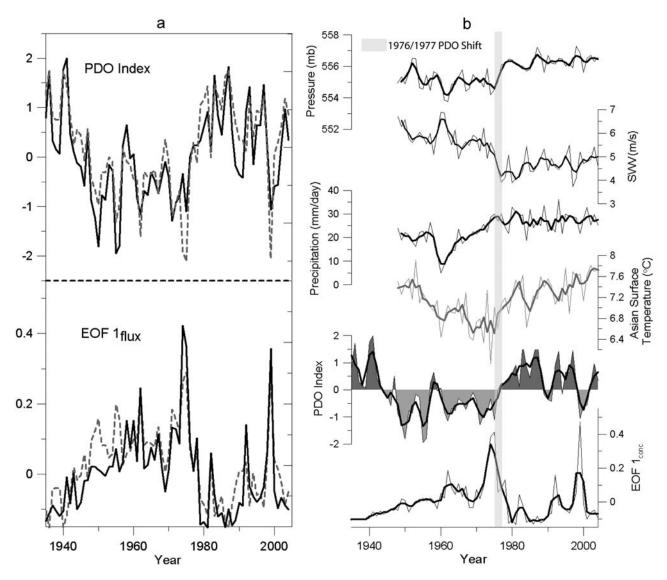
Figure 7. (a) Plots of the Pacific Decadal Oscillation (PDO) index and EOF 1_{flux} (solid line) and their common EOF 1 (dashed shaded line). For negative correlations (e.g., EOF 1_{flux}), the EOF is oriented inversely. (b) NCEP/NCAR reanalysis: Mt. Geladaindong grid (pressure, scalar wind velocity, and precipitation), Asian surface temperature ($10.0°-70.0°$N; $70.0°-105.0°$E), annual PDO index (see http://jisao.washington.edu/pdo/PDO.latest), and EOF $1_{conc.}$ 3-year running mean (bold lines) and 1-year mean (thin lines) of the annual average.

2001; *MacDonald and Case*, 2005]; however, PDO reconstruction studies for Asia are very limited [*D'Arrigo and Wilson*, 2006]. Although PDO reconstructions are scarce, recent research suggests that the Asian climate plays an important role in the PDO. The PDO is thought to interact with the Asian monsoon, and North Pacific SST anomalies have been correlated with eastern Asian climate extremes [*Chan and Zhou*, 2005; *Chongyin et al.*, 2004; *Lau et al.*, 2004; *Nakamura et al.*, 2002]. PDO regime shifts have been related to interdecadal trends of precipitation and air temperature in north central China [*Ma*, 2007] and Japanese coastal air temperature [*Minobe*, 1997]. *Frauenfeld and Davis* [2002] suggest that the 1976 regime shift may have been a result of recent Asian landmass heating, implying that the Eurasian atmosphere may have a strong influence on decadal Pacific SST variability.

[21] Comparison between the annual PDO index (http://jisao.washington.edu/pdo/PDO.latest) and annual EOF $1_{conc.}$ and EOF 1_{flux} suggest that there is a teleconnection between the PDO and atmospheric crustal aerosols on the TP. A relationship is most prominently suggested by the abrupt shifts in trends during the mid-1970s in the PDO and EOF $1_{conc. and flux}$ time series (Figures 7a and 7b). EOF analysis revealed that ~71% (EOF $1_{conc.}$) and ~73% (EOF 1_{flux}) of the variance with the PDO index series was represented by the first EOF (negative correlation). The close correspondence between the PDO Index and the potential proxy (EOF 1) is shown in Figure 7a where their first common component (EOF 1) is shown as a dashed gray line. The linear correlation coefficient between the EOF $1_{conc. and flux}$ and the PDO Index time series revealed a significant relationship (conc.: $r = -0.42, p < 0.0001, n = 70$;
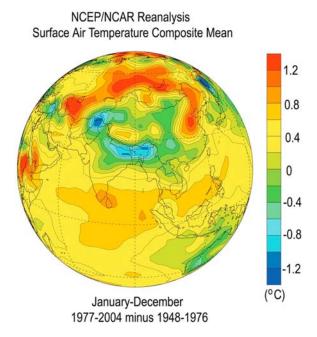
NCEP/NCAR Reanalysis
Surface Air Temperature Composite Mean

January-December
1977-2004 minus 1948-1976

(°C)

Figure 8. Annual surface temperature differences between 1948 and 1976 and 1977–2004.

flux: $r = -0.46$, $p < 0.0001$, $n = 70$). This inverse relationship suggests that negative PDO values correspond to higher atmospheric soluble dust aerosols at Mt. Geladaindong. The 1947–1976 PDO negative phase coincided with overall lower pressure, higher SWV, and higher soluble dust aerosol concentrations, while the 1977–2004 positive phase coincides with higher pressure, lower wind velocities, and lower soluble dust aerosol concentrations suggesting a multidecadal relationship (Figure 7b). It is interesting to note that the anomalously high soluble aerosol concentrations in 1999 coincide with an abrupt negative year in the PDO. Examination of 1999 NCEP/NCAR reanalysis climate variables showed a decrease in precipitation over the Mt. Geladaindong region, which may explain increased atmospheric soluble dust as a product of dryer, more readily entrained particles and reduced atmospheric scavenging. Similar correlations were conducted with the North Atlantic Oscillation (NAO), Atlantic Multidecadal Oscillation (AMO), and Southern Oscillation Index (SOI). NAO (http://cdc.noaa.gov/gcos_wgsp/Timeseries/Data/nao.dat) and AMO (http://cdc.noaa.gov/data/correlation/amon.us. data) reported no significant values ($p > 0.05$); however, the SOI (http://born.gov.au/climate/glossary/soi.shtml) displayed significant correlations (EOF $1_{conc.}$: $r = -0.26$, $p < 0.0001$, $n = 70$; EOF 1_{flux}: $r = -0.29$, $p < 0.0001$, $n = 70$) that are weaker overall than the PDO correlations. The similarity in significant correlations in not surprising considering the teleconnection between the PDO and El Niño–Southern Oscillation [*McCabe and Dettinger*, 1999].

4.4. Shifts in Atmospheric Dust Concentrations and the Warming of Asia

[22] Annual surface temperature differences between 1948 and 1976 and 1977–2004 indicate that northern Asia and regions of the TP have experienced warmer temperatures since 1977 (Figure 8). The reconstructed temperature series from the Mt. Geladaindong $\delta^{18}O$ ice core record is consistent with recent regional Tibetan Plateau and Northern Hemisphere warming [*Kang et al.*, 2007]. Examination of NCEP/NCAR reanalysis average annual surface air temperature trends over a large portion of the Asian continent ($10.0° - 70.0°N$; $70.0° - 105.0°E$) suggests a relationship between the PDO, Asian landmass warming, and Mt. Geladaindong EOF $1_{conc.\ and\ flux}$ (i.e., soluble dust) which are all highlighted by concurrent mid-1970s shifts (Figure 7b). The relationship between Asian landmass warming and atmospheric dust concentrations on the TP may be explained by reductions in regional temperature gradients that reduce regional pressure gradients. Regional pressure gradients are the dominant control on cyclonic systems and wind velocity strengths: two of the primary factors in dust entrainment and transport.

[23] Whether this warming in Asia is partly a response to or cause of the PDO shift is not yet clear, although it has been suggested that decadal Pacific SST variability could be forced by the atmosphere over Eurasia and that the 1976/1977 PDO shift is a response of recent Asian landmass heating [*Frauenfeld and Davis*, 2002]. Regardless of the cause, the correlation between Mt. Geladaindong EOF $1_{conc.\ and\ flux}$ and the PDO index suggests that EOF $1_{conc.\ and\ flux}$ may be used as a proxy to reconstruct the PDO using longer Mt. Geladaindong ice cores and thereby potentially enhancing the understanding of PDO mechanisms.

5. Conclusions

[24] This paper presents the atmospheric soluble dust history between 1935 and 2004 from an ice core from Mt. Geladaindong on the TP. Annual interspecies major soluble ion correlations and EOF analysis suggest that Mt. Geladaindong has multiple dust sources. Major soluble ion time series show an abrupt threefold decrease in concentrations during the mid-1970s corresponding to major shifts in NCEP/NCAR reanalysis surface pressure and SWV. EOF analysis and linear correlations between Mt. Geladaindong EOF $1_{conc.\ and\ flux}$ and NCEP/NCAR reanalysis climate variables suggest that the EOF $1_{conc.\ and\ flux}$ records may be a proxy for surface pressure (cyclonic storm activity). Mt. Geladaindong EOF $1_{conc.\ and\ flux}$ records also demonstrated a significant negative correlation with the PDO Index, indicating that the PDO may be teleconnected to dust entrainment on the TP. The relationship is most prominent during the 1976/1977 PDO phase shift, which coincides with a large and abrupt decrease in EOF $1_{conc.\ and\ flux}$ values (i.e., soluble dust concentrations). Investigation of regional climate variable trends with the PDO Index showed potential relationships between the 1976/1977 PDO phase shift and major shifts in regional surface pressure and SWV on the TP. The large increase in overall Asian landmass annual temperature trends during the 1970s also coincided with the 1976/1977 PDO shift. Late-20th-century warming over Asia and resultant reductions in regional temperature gradients may have weakened pressure gradients responsible for cyclonic activity and wind strength, the two primary components of dust entrainment and transport. The results from the 70-yearlong Mt. Geladaindong ice core suggest

that longer records hold potential to reconstruct a PDO Index for central Asia.

References

Aizen, V., E. Aizen, J. Melack, and T. Martma (1996), Isotopic measurements of precipitation on central Asian glaciers (southeastern Tibet, northern Himalayas, central Tien Shan), *J. Geophys. Res.*, *101*, 9185–9196, doi:10.1029/96JD00061.

Aizen, V., E. Aizen, J. Melack, K. Kreutz, and L. Cecil (2004), Association between atmospheric circulation patterns and firn-ice core records from the Inilchek glacierized area, central Tien Shan, Asia, *J. Geophys. Res.*, *109*, D08304, doi:10.1029/2003JD003894.

Anspaugh, L., et al. (2000), *Report of the United Nations Scientific Committee on the Effects of Atomic Radiation to the General Assembly*, United Nations, New York.

Biondi, F., A. Gershunov, and D. Cayan (2001), North Pacific decadal climate variability since AD 1661, *J. Clim.*, *14*, 5–10, doi:10.1175/1520-0442(2001)014<0005:NPDCVS>2.0.CO;2.

Bryson, R. A. (1986), Airstream climatology of Asia, in *Proceedings of the International Symposium on the Qinghai-Xizang Plateau and Mountain Meteorology*, pp. 604–617, Am. Meteorol. Soc., Boston, Mass.

Chan, J. C. L., and W. Zhou (2005), PDO, ENSO and the early summer monsoon rainfall over south China, *Geophys. Res. Lett.*, *32*, L08810, doi:10.1029/2004GL022015.

Chongyin, L., H. Jinhai, and Z. Jinhong (2004), A review of decadal/interdecadal climate variation studies in China, *Adv. Atmos. Sci.*, *21*, 425–436, doi:10.1007/BF02915569.

Claquin, T., M. Schulz, and Y. J. Balkanski (1999), Modeling the mineralogy of atmospheric dust sources, *J. Geophys. Res.*, *104*, 22,243–22,256, doi:10.1029/1999JD900416.

Cong, Z., S. Kang, X. Liu, and G. Wang (2007), Elemental composition of aerosol in the Nam Co region, Tibetan Plateau, during summer monsoon season, *Atmos. Environ.*, *41*, 1180–1187, doi:10.1016/j.atmosenv.2006.09.046.

Cook, E. (2002), Reconstructions of Pacific decadal variability from long tree-ring records, *Eos Trans. AGU*, *83*(19), Spring Meet. Suppl., Abstract GC42A-04.

D'Arrigo, R., and R. Wilson (2006), On the Asian expression of the PDO, *Int. J. Climatol.*, *26*, 1607–1617, doi:10.1002/joc.1326.

D'Arrigo, R., R. Villalba, and G. Wiles (2001), Tree-ring estimates of Pacific decadal climate variability, *Clim. Dyn.*, *18*, 219–224, doi:10.1007/s003820100177.

Fang, X., Y. Han, and J. Ma (2004), Characteristics of dust storm and loess sediment in the Tibetan Plateau: A case study of dust event on Mar. 4, 2003 in Lhasa, *Chin. Sci. Bull.*, *49*, 1084–1090.

Frauenfeld, O., and R. Davis (2002), Midlatitude circulation patterns associated with decadal and interannual Pacific Ocean variability, *Geophys. Res. Lett.*, *29*(24), 2221, doi:10.1029/2002GL015743.

Gedalof, Z., and D. Smith (2001), Interdecadal climate variability and regime-scale shifts in Pacific North America, *Geophys. Res. Lett.*, *28*, 1515–1518, doi:10.1029/2000GL011779.

Gong, S. L., X. Y. Zhang, T. L. Zhao, and L. A. Barrie (2004), Sensitivity of Asian dust storm to natural and anthropogenic factors, *Geophys. Res. Lett.*, *31*, L07210, doi:10.1029/2004GL019502.

Han, Y., X. Xi, and L. Song (2004), Spatio-temporal sand-dust distribution in Qinghai-Tibet Plateau and its climatic significance, *J. Desert Res.*, *24*, 588–592.

Huang, J., P. Minnis, Y. Yi, Q. Tang, X. Wang, Y. Hu, Z. Liu, K. Ayers, C. Trepte, and D. Winker (2007), Summer dust aerosols detected from CALIPSO over the Tibetan Plateau, *Geophys. Res. Lett.*, *34*, L18805, doi:10.1029/2007GL029938.

Institute of Soil Science of Academia Sinica (1985), *Soils of Tibet*, Sci. Press, Beijing.

Jacobson, M. Z. (2005), *Fundamentals of Atmospheric Modeling*, Cambridge Univ. Press, Cambridge, U. K.

Kalnay, E., et al. (1996), The NCEP/NCAR 40-year reanalysis project, *Bull. Am. Meteorol. Soc.*, *77*, 437–470, doi:10.1175/1520-0477(1996)077<0437:TNYRP>2.0.CO;2.

Kang, S. C., D. H. Qin, P. A. Mayewski, C. P. Wake, and J. W. Ren (2001), Climatic and environmental records from the Far East Rongbuk ice core, Mt. Qomolangma (Mt. Everest), *Episodes*, *24*, 176–181.

Kang, S., P. A. Mayewski, D. Qin, Y. Yan, S. Hou, D. Zhang, J. Ren, and K. Kruetz (2002a), Glaciochemical records from a Mt. Everest ice core: Relationship to atmospheric circulation over Asia, *Atmos. Environ.*, *36*, 3351–3361, doi:10.1016/S1352-2310(02)00325-4.

Kang, S. C., P. A. Mayewski, D. H. Qin, Y. P. Yan, D. Q. Zhang, S. G. Hou, and J. W. Ren (2002b), Twentieth century increase of atmospheric ammonia recorded in Mount Everest ice core, *J. Geophys. Res.*, *107*(D21), 4595, doi:10.1029/2001JD001413.

Kang, S., Y. Zhang, D. Qin, J. Ren, Q. Zhang, B. Grigholm, and P. A. Mayewski (2007), Recent temperature increase recorded in an ice core in the source region of Yangtze River, *Chin. Sci. Bull.*, *52*, 825–831, doi:10.1007/s11434-007-0140-1.

Kaspari, S., et al. (2007), Reduction in northward incursions of the South Asian monsoon since ~1400 AD inferred from a Mt. Everest ice core, *Geophys. Res. Lett.*, *34*, L16701, doi:10.1029/2007GL030440.

Kreutz, K. J., and E. R. Sholkovitz (2000), Major element, rare Earth element, and sulfur isotopic composition of a high-elevation firn core: Sources and transport of mineral dust in central Asia, *Geochem. Geophys. Geosyst.*, *1*(11), 1048, doi:10.1029/2000GC000082.

Kreutz, K. J., V. B. Aizen, L. D. Cecil, and C. P. Wake (2001), Oxygen isotopic and soluble ionic composition of a shallow firn core, Inilchek Glacier, central Tien Shan, *J. Glaciol.*, *47*, 548–554, doi:10.3189/172756501781831819.

Lau, K., J. Lee, K. Kim, and I. Kang (2004), The North Pacific as a regulator of summer climate over Eurasia and North America, *J. Clim.*, *17*, 819–833, doi:10.1175/1520-0442(2004)017<0819:TNPAAR>2.0.CO;2.

Laurent, B., B. Marticorena, G. Bergametti, and F. Mei (2006), Modeling mineral dust emissions from Chinese and Mongolian deserts, *Global Planet. Change*, *52*, 121–141, doi:10.1016/j.gloplacha.2006.02.012.

Li, C., S. Kang, Q. Zhang, and S. Kaspari (2007), Major ionic composition of precipitation in the Nam Co region, central Tibetan Plateau, *Atmos. Res.*, *85*, 351–360, doi:10.1016/j.atmosres.2007.02.006.

Li, M., S. Kang, L. Zhu, Q. You, Q. Zhang, and J. Wang (2008), Mineralogy and geochemistry of the Holocene lacustrine sediments in Nam Co, Tibet, *Quat. Int.*, *187*, 105–116, doi:10.1016/j.quaint.2007.12.008.

Li-Jones, X., and J. M. Prospero (1998), Variations in the size distribution of non-sea-salt sulfate aerosol in the marine boundary layer at Barbados: Impact of African dust, *J. Geophys. Res.*, *103*, 16,073–16,084, doi:10.1029/98JD00883.

Liu, X., and B. Chen (2000), Climatic warming in the Tibetan Plateau during recent decades, *Int. J. Climatol.*, *20*, 1729–1742, doi:10.1002/1097-0088(20001130)20:14<1729::AID-JOC556>3.0.CO;2-Y.

Liu, Z., et al. (2008), Airborne dust distributions over the Tibetan Plateau and surrounding areas derived from the first year of CALIPSO lidar observations, *Atmos. Chem. Phys.*, *8*, 5045–5060.

Lyons, W. B., and P. A. Mayewski (1983), Nitrate plus nitrite concentrations in a Himalayan ice core, *Geophys. Res. Lett.*, *10*, 1160–1163, doi:10.1029/GL010i012p01160.

Ma, Z. (2007), The interdecadal trend and shift of dry/wet over the central part of north China and their relationship to the Pacific Decadal Oscillation (PDO), *Chin. Sci. Bull.*, *52*, 2130–2139, doi:10.1007/s11434-007-0284-z.

MacDonald, G., and R. Case (2005), Variations in the Pacific Decadal Oscillation over the past millennium, *Geophys. Res. Lett.*, *32*, L08703, doi:10.1029/2005GL022478.

Mayewski, P. A., W. B. Lyons, and N. Ahmad (1983), Chemical composition of a high altitude fresh snowfall in the Ladakh Himalayas, *Geophys. Res. Lett.*, *10*, 105–108, doi:10.1029/GL010i001p00105.

Mayewski, P. A., W. B. Lyons, N. Ahmad, G. Smith, and M. Pourchet (1984), Interpretation of the chemical and physical time-series retrieved from Sentik Glacier, Ladakh, Himalaya, India, *J. Glaciol.*, *30*, 66–76.

Mayewski, P. A., et al. (2004), A 700 year record of Southern Hemisphere extratropical climate variability, *Ann. Glaciol.*, *39*, 127–132, doi:10.3189/172756404781814249.

McCabe, G. J., and M. D. Dettinger (1999), Decadal variations in the strength of ENSO teleconnections with precipitation in the western United States, *Int. J. Climatol.*, *19*, 1399–1410, doi:10.1002/(SICI)1097-0088(19991115)19:13<1399::AID-JOC457>3.0.CO;2-A.

Meeker, L. D., and P. A. Mayewski (2002), A 1400-year high-resolution record of atmospheric circulation over the North Atlantic and Asia, *Holocene*, *12*, 257–266, doi:10.1191/0959683602hl542ft.

Merrill, J. T., M. Uematsu, and R. Bleck (1989), Meteorological analysis of long range transport of mineral aerosol over the North Pacific, *J. Geophys. Res.*, *94*, 8584–8598, doi:10.1029/JD094iD06p08584.

Minobe, S. (1997), A 50–70 year climatic oscillation over the North Pacific and North America, *Geophys. Res. Lett.*, *24*, 683–686, doi:10.1029/97GL00504.

Nakamura, H., T. Izumi, and T. Sampe (2002), Interannual and decadal modulations recently observed in the Pacific storm track activity and East Asian winter monsoon, *J. Clim.*, *15*, 1855–1874, doi:10.1175/1520-0442(2002)015<1855:IADMRO>2.0.CO;2.

Osterberg, E. C., M. J. Handley, S. B. Sneed, P. A. Mayewski, and K. J. Kreutz (2006), Continuous ice core melter system with discrete sampling for major ion, trace element, and stable isotope analyses, *Environ. Sci. Technol.*, *40*, 3355–3361, doi:10.1021/es052536w.

Pruppacher, H. R., and J. D. Klett (1978), *Microphysics of Clouds and Precipitation*, Kluwer Acad., Norwell, Mass.

Qian, W., L. Quan, and S. Shi (2002), Variations of the dust storm in China and its climatic control, *J. Clim.*, *15*, 1216–1229, doi:10.1175/1520-0442(2002)015<1216:VOTDSI>2.0.CO;2.

Qin, D. H., P. A. Mayewski, S. C. Kang, J. W. Ren, S. G. Hou, T. D. Yao, Q. Z. Yang, Z. F. Jin, and D. S. Mi (2000), Evidence for recent climate change from ice cores in the central Himalaya, *Ann. Glaciol.*, *31*, 153–158, doi:10.3189/172756400781819789.

Qin, D. H., S. G. Hou, D. Q. Zhang, J. W. Ren, S. C. Kang, P. A. Mayewski, and C. P. Wake (2002), Preliminary results from the chemical records of an 80.4 m ice core recovered from East Rongbuk Glacier, Qomolangma (Mount Everest), Himalaya, *Ann. Glaciol.*, *35*, 278–284, doi:10.3189/172756402781816799.

Shrestha, A. B., C. P. Wake, J. E. Dibb, and S. I. Whitlow (2002), Aerosol and precipitation chemistry at a remote Himalayan site in Nepal, *Aerosol Sci. Technol.*, *36*, 441–456, doi:10.1080/027868202753571269.

Tegen, I., A. A. Lacis, and I. Fung (1996), The influence on climate forcing of mineral aerosols from disturbed soils, *Nature*, *380*, 419–422, doi:10.1038/380419a0.

Thompson, L. G., E. Mosley-Thompson, M. E. Davis, J. F. Bolzan, J. Dai, T. Yao, N. Gundestrup, X. Wu, L. Klein, and Z. Xie (1989), Holocene–Late Pleistocene climatic ice core records from Qinghai-Tibetan Plateau, *Science*, *246*, 474–477, doi:10.1126/science.246.4929.474.

Thompson, L. G., E. Mosley-Thompson, M. Davis, P. N. Lin, T. Yao, M. Dyurgerov, and J. Dai (1993), "Recent warming": Ice core evidence from tropical ice cores with emphasis on central Asia, *Global Planet. Change*, *7*, 145–156, doi:10.1016/0921-8181(93)90046-Q.

Thompson, L. G., E. Mosley-Thompson, M. E. Davis, P. N. Lin, K. A. Henderson, J. Cole-Dai, J. F. Bolzan, and K. B. Liu (1995), Late Glacial Stage and Holocene tropical ice core records from Huscaran, Peru, *Science*, *269*, 46–50, doi:10.1126/science.269.5220.46.

Thompson, L. G., V. Mikhalenko, E. Mosley-Thompson, M. Durgerov, P. N. Lin, M. Moskalevsky, M. E. Davis, S. Arkhipov, and J. Dai (1997), Ice core records of recent climatic variability: Grigoriev and It-Tish ice caps in central Tien Shan, central Asia, *Mater. Glyatsiol. Issled.*, *81*, 100–109.

Thompson, L. G., T. Yao, E. Mosley-Thompson, M. E. Davis, K. A. Henderson, and P. N. Lin (2000), A high-resolution millennial record of the South Asian monsoon from Himalayan ice cores, *Science*, *289*, 1916–1919, doi:10.1126/science.289.5486.1916.

Tian, L., V. Masson-Delmotte, M. Stievenard, T. Yao, and J. Jouzel (2001), Tibetan Plateau summer monsoon northward extent revealed by measurements of water stable isotopes, *J. Geophys. Res.*, *106*, 28,081–28,088, doi:10.1029/2001JD900186.

Wake, C. P., P. A. Mayewski, and M. J. Spencer (1990), A review of central Asian glaciochemical data, *Ann. Glaciol.*, *14*, 301–306.

Wake, C. P., P. A. Mayewski, Z. C. Xie, P. Wang, and Z. Q. Li (1993), Regional distribution of monsoon and desert dust signals recorded in Asian glaciers, *Geophys. Res. Lett.*, *20*, 1411–1414, doi:10.1029/93GL01682.

Wake, C. P., P. A. Mayewski, Z. Li, J. Han, and D. Qin (1994), Modern eolian dust deposition in central Asia, *Tellus, Ser. B*, *46*, 220–233, doi:10.1034/j.1600-0889.1994.t01-2-00005.x.

Wang, G., Y. Shen, and G. Cheng (2000a), Eco-environmental changes and causal analysis in the source regions of the Yellow River (in Chinese), *J. Glaciol. Geocryol.*, *22*, 200–206.

Wang, S., H. Jin, S. Li, and L. Zhao (2000b), Permafrost degradation on the Qinghai-Tibet Plateau and its environmental impacts, *Permafrost Periglacial Processes*, *11*, 43–53, doi:10.1002/(SICI)1099-1530(200001/03)11:1<43::AID-PPP332>3.0.CO;2-H.

Wu, S., and Q. Yang (2000), Land-use and agricultural development, in *Mountain Genecology and Sustainable Development of the Tibetan Plateau*, edited by D. Zheng, Q. Zhang, and S. Wu, pp. 181–202, Kluwer Acad., Dordrecht, Netherlands.

Xie, A., J. Ren, X. Qin, and S. Kang (2007), Reliability of NCEP/NCAR reanalysis data in the Himalayas/Tibetan Plateau, *J. Geogr. Sci.*, *17*, 421–430, doi:10.1007/s11442-007-0421-2.

Zeng, Y., Z. Feng, and G. Cao (2003), Land cover change and its environmental impact in the upper reaches of the Yellow River, northeast Qinghai–Tibetan Plateau, *Mt. Res. Dev.*, *23*, 353–361, doi:10.1659/0276-4741(2003)023[0353:LCCAIE]2.0.CO;2.

Zhang, X. Y., Z. Shen, G. Zhang, T. Chen, and H. Liu (1996), Remote mineral aerosol in westerlies and their contributions to Chinese loess, *Sci. China, Ser. D*, *39*, 67–76.

Zhang, X. Y., R. Arimoto, and Z. S. An (1997), Dust emission from Chinese desert sources linked to variations in atmospheric circulation, *J. Geophys. Res.*, *102*, 28,041–28,047, doi:10.1029/97JD02300.

Zhang, X. Y., R. Arimoto, J. J. Cao, Z. S. An, and D. Wang (2001), Atmospheric dust aerosol over the Tibetan Plateau, *J. Geophys. Res.*, *106*, 18,471–18,476, doi:10.1029/2000JD900672.

Zhang, Y., and G. R. Carmichael (1999), The role of mineral aerosol in tropospheric chemistry in East Asia: A model study, *J. Appl. Meteorol.*, *38*, 353–366, doi:10.1175/1520-0450(1999)038<0353:TROMAI>2.0.CO;2.

Zhang, Y., S. C. Kang, Q. G. Zhang, Z. Cong, and Y. Zhang (2008), Microparticle variations in snowpits from Mt. Geladaindong in the source region of Yangtze River and its environmental significance, *Environ. Sci.*, *29*, 2117–2122.

Zhong, D. C. (1999), The dynamic changes and trends of modern desert in China, *Adv. Earth Sci.*, *14*, 229–234.

Zhu, J. F., and Z. D. Zhu (1999), *Combating Desertification in China*, China For. Press, Beijing.

────────────────

B. Grigholm, S. Kaspari, P. A. Mayewski, and S. B. Sneed, Climate Change Institute, Department of Earth Sciences, University of Maine, 134 Sawyer Environmental Research Center, Orono, ME 04469, USA. (bjorn.grigholm@maine.edu)

S. Kang, Q. Zhang, and Y. Zhang, Institute of Tibetan Plateau Research, Chinese Academy of Sciences, Beijing 100085, China.